Hyperbolic Chaos of Turing Patterns

Pavel V. Kuptsov,[1,*] Sergey P. Kuznetsov,[2] and Arkady Pikovsky[3]

[1]*Department of Instrumentation Engineering, Saratov State Technical University, Politekhnicheskaya 77, Saratov 410054, Russia*

[2]*Kotel'nikov's Institute of Radio-Engineering and Electronics of RAS, Saratov Branch, Zelenaya 38, Saratov 410019, Russia*

[3]*Institute of Physics and Astronomy, University of Potsdam, Karl-Liebknecht-Strasse 24/25, 14476 Potsdam-Golm, Germany*

(Received 19 January 2012; revised manuscript received 27 February 2012; published 7 May 2012)

We consider time evolution of Turing patterns in an extended system governed by an equation of the Swift-Hohenberg type, where due to an external periodic parameter modulation longwave and shortwave patterns with length scales related as 1:3 emerge in succession. We show theoretically and demonstrate numerically that the spatial phases of the patterns, being observed stroboscopically, are governed by an expanding circle map, so that the corresponding chaos of Turing patterns is hyperbolic, associated with a strange attractor of the Smale-Williams solenoid type. This chaos is shown to be robust with respect to variations of parameters and boundary conditions.

DOI: 10.1103/PhysRevLett.108.194101 PACS numbers: 89.75.Kd, 05.45.Jn

In nonlinear dynamics the notion of structural stability, or robustness, is one of the key tools allowing one to specify systems and effects that are really significant for theoretical and numerical researches, and especially for practical applications [1,2]. Among chaotic attractors, structural stability is intrinsic to those possessing the uniform hyperbolicity (''the systems with axiom A''), mathematical examples of which were advanced already since the 1960s and 1970s [3–6]. At that time, such attractors were expected to be relevant for various physical situations (such as hydrodynamic turbulence), but later it became clear that the chaotic attractors, which normally occur in applications, do not relate to the class of structurally stable ones. This is an obvious contradiction to the principle of significance of the robust systems mentioned above.

Recently, this inconsistency has been partially resolved by introducing a number of physically realizable systems with hyperbolic chaotic attractors [7–10]. It has been shown that simple systems of coupled oscillators that are excited alternately (in time) possess hyperbolic attractors of Smale-Williams type (for experimental realizations, see [9–11]). Hyperbolic chaos in these systems is related to the dynamics of the phases of the oscillators, evolution of which on the successive stages of activity is governed by a Bernoulli-type expanding circle map.

In this Letter we develop a similar approach, but deal with the spatial phases of patterns in a spatially extended system. We demonstrate the occurrence of hyperbolic chaos in dynamics resulting from an interplay of two Turing patterns of different wavelengths arising in succession. This advance, first, extends a toolbox for design of models manifesting robust chaos. Second, it suggests a novel direction for search of situations associated with hyperbolic chaos in the context, e.g., of fluid turbulence, convection, and reaction-diffusion systems. Third, the description in terms of truncated equations for amplitudes of spatial modes leads to new prototypical low-dimensional model systems with hyperbolic attractors. (Note analogy with the Lorenz equations, which were derived originally as a finite-dimensional model for fluid convection.)

Let us illustrate the approach with a concrete example based on the one-dimensional Swift-Hohenberg equation [12]. Consider its following modification:

$$\partial_t u + [1 + \kappa^2(t)\partial_x^2]^2 u = [A + B\chi(x)]u - u^3. \quad (1)$$

Here A is a positive parameter controlling the Turing instability. An instant value of κ determines the wave number of the unstable Turing mode. In our case $\kappa(t)$ is assumed to be a periodic function: $\kappa(t) = 1$ for $nT \le t < (n + 1/2)T$, and $\kappa(t) = 1/3$ for $(n + 1/2)T \le t < (n + 1)T$. This switching provides the excitation of two distinct alternating in time Turing patterns characterized by the dominating wave numbers, $k = 1$ and $k = 3$, respectively. The time interval T between the switchings is supposed to exceed the characteristic time duration of the formation or decay of the Turing patterns. A nonlinear cubic term in the equation is responsible for saturation of the instability. Also, the coefficient at the linear term in the equation is assumed to depend on the spatial coordinate that corresponds to the presence of a spatial nonuniformity characterized by a function $\chi(x)$; its role will be clarified below. Assuming the ring geometry and periodic boundary conditions $u(x, t) \equiv u(x + L, t)$ (PBC), it is natural to set the length of the system as $L = 2\pi\ell$, with integer ℓ, to get the geometry supporting the Turing patterns of both the wave numbers $k = 1$ and 3.

The system operates as follows. In each time interval with $\kappa(t) = 1$ the Turing pattern with the dominating wave number $k = 1$ arises, which is characterized by some

spatial phase φ: $u \sim U_1 \cos(x + \varphi) + \tilde{U}_3 \cos(3x + 3\varphi)$, where $\tilde{U}_3 \ll U_1$, and U_1 is of the order of $\sqrt{A}$. (The third harmonic appears naturally due to the cubic nonlinear term in the equation.) After the switch to $\kappa = 1/3$ the system becomes unstable in respect to the harmonic component with $k = 3$, while that with $k = 1$ starts to decay. The initial stimulation of the shortwave pattern is provided by the component $\tilde{U}_3$; so, it accepts the spatial phase 3φ. At the end of the considered time interval the first harmonic component practically disappears, and we have $u \sim U_3 \cos(3x + 3\varphi)$, with U_3 of the order of $\sqrt{A}$. After the next switch, when $\kappa = 1$ again, the third harmonic decays, but the first harmonic becomes unstable and starts to grow. A germ for this growth is provided by a component at the wave number $k = 1$ arising from the combination of the decaying shortwave pattern and the spatially dependent coefficient $\chi(x)$. If the Fourier expansion of $\chi(x)$ contains a dominating second harmonic $k = 2$, the longwave mode will arise with the phase 3φ, due to the term proportional to $\cos 2x \cos(3x + 3\varphi) = (1/2)\cos(x + 3\varphi) + \ldots$. Thus, on each complete period of modulation T the phase of the spatial pattern undergoes the tripling (up to a constant phase shift): $\varphi_{n+1} = 3\varphi_n + \text{const}$. This is an expanding circle map with chaotic behavior characterized by the positive Lyapunov exponent $\Lambda = \ln 3 \approx 1.0986$ [13]. Since the phase map is uniformly expanding, the stroboscopic map corresponding to the transformation of the states $u_n(x) \equiv u(x, t_n)$ from $t_n = nT + \text{const}$ to t_{n+1} is expected to be hyperbolic.

Of course, this mode of operation occurs under the proper choice of the parameters. A value of A is selected to get an instability at $k = 1$ with a decay at $k = 3$, or vice versa, at successive half-periods of parameter modulation. The term $B\chi(x)$ must be small (comparing to the fully developed pattern amplitude) to contribute only as a germ for the formation of the longwave pattern, although this germ should be of a sufficient level to start the process with saturation on the time scale T. In fact, the requirements are not very strict: the described type of behavior occurs in a fairly wide parameter range.

Figure 1 illustrates the spatiotemporal behavior of the system observed for the case of PBC. The 3D-plot $u(x, t)$ is obtained using computations on a spatial grid with the node separation $\Delta x = L/N$, where N is a number of the nodes. One can observe the alternating evolution of the Turing structures: a longwave pattern first appears, then decays, and is replaced by a shortwave one. After the period T, the longwave pattern reappears but with a different spatial phase (shift along x axis), and the process repeats. As we show in Fig. 2(a), the spatial phases recorded stroboscopically follow a chaotic map of the expected type. To obtain this diagram, we determine the spatial phases at $t_n = (n + 1/4)T$ as $\varphi_n = \arg[u(L/2, t_n) + i\partial_x u(L/2, t_n)]$, where the spatial derivative $\partial_x u$ is estimated by the numerical differentiation, and the results are plotted in coordinates φ_{n+1} versus φ_n. This empirical map is of the expected topological type: one revolution for the preimage corresponds to three revolutions for the image.

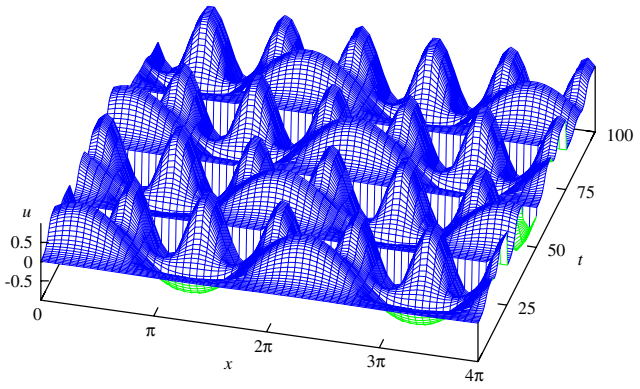

FIG. 1 (color online). Hyperbolically chaotic patterns in model (1) at $A = 0.6$, $B = 0.03$, $T = 25$, $L = 4\pi$, $N = 64$, PBC.

To characterize chaos quantitatively and demonstrate its robustness, we calculate the Lyapunov exponents. Figure 3(a) shows the first five Lyapunov exponents for the stroboscopic map as functions of the parameter A. The chaotic mode of operation occurs above some threshold around $A \approx 0.38$. In the chaotic regime there is one positive Lyapunov exponent, which remains almost constant in a wide parameter range. In particular, at $A = 0.6$ the Lyapunov exponents are $\Lambda = \{1.018, -9.34, -9.34, -11.42, -18.64, \ldots\}$. As expected, the largest exponent is close to ln3. As seen from the diagram, all the exponents depend on the parameter smoothly, without sharp spikes or dips. This is a manifestation of robustness of the hyperbolic chaos [7,9,10]. The Kaplan-Yorke dimension of the attractor varies slightly, see the solid line in Fig. 3(b); in particular $D_{\mathrm{KY}} \approx 1.11$ at $A = 0.6$.

To confirm the validity of the used spatial discretization, in Fig. 3(c) we show the 16 largest Lyapunov exponents obtained at a fixed length L with different sizes of the numerical mesh N. The decrease of $\Delta x = L/N$ corresponds obviously to approaching the continuous limit. The left-hand parts of the curves overlap perfectly; so, the larger exponents are in good correspondence for all

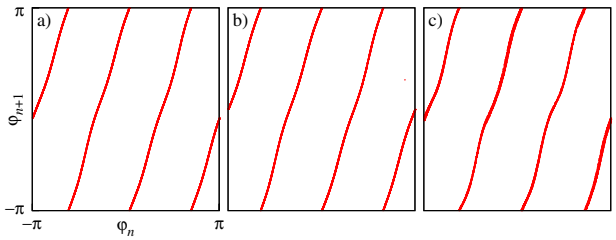

FIG. 2 (color online). Diagrams for spatial phases of Turing patterns at $t_n = (n + 1/4)T$ for $A = 0.6$, $B = 0.03$, $T = 25$. (a) Numerical solution of the system (1), PBC, $L = 4\pi$, $N = 64$. (b) Amplitude equations (3). (c) System (1) with ZBC, $L = 8\pi$, $N = 128$.

tested step sizes. The discrepancy visible in the right-hand part of the plot for large negative exponents decreases with the growth of N. Hence, we can be sure that the properties revealed in the computations with the finite discretization size are valid for the continues system as well.

Next, we perform a direct test of the hyperbolicity. The hyperbolicity implies that there are no tangencies between the stable and unstable manifolds of orbits belonging to the attractor. Occurrence of a tangency is determined by the zero angle between the expanding and contracting tangent subspaces spanned by the corresponding covariant Lyapunov vectors [14]. Following the method for testing hyperbolicity described in [15], we examine the distribution of these angles by considering the orthogonal complement to the contracting subspace, which is normally much less dimensional then the contracting subspace itself. If there are K expanding directions, it is sufficient to calculate K orthogonal backward and forward Lyapunov vectors, to construct a $K \times K$ matrix $\mathbf{P}$ of their scalar products, and to check how close to zero is the normalized characteristic number

$$d_K = |\det(\mathbf{P})|. \tag{2}$$

By the definition, $0 \le d_K \le 1$. The procedure is applied at a representative set of points on a trajectory on the attractor. The distribution of d_K separated well from zero means that the chaos is detected as hyperbolic: the tested trajectory does not contain any points with tangencies of the expanding and conracting Lyapunov vectors.

In application to the stroboscopic map of the system (1) the calculations are simple because $K = 1$. For the parameters used in Fig. 1 we processed 10^5 points and observed that $(1 - 5 \times 10^{-5}) < d_1 \le 1$. It means that the expanding direction is always almost orthogonal to the contracting subspace. Thus, the conjecture that the attractor is uniformly hyperbolic is confirmed, but, of course, a rigorous mathematical proof of the hyperbolicity would be desirable anyway.

As in the system only two modes with the wave numbers $k = 1$ and $k = 3$ are basically involved, one can expect that the essential properties of the dynamics can be described with a truncated model. To derive the low-dimensional model we proceed as follows. Accounting for the relevant modes, we use the ansatz $u = a_1(t) \times \cos x + b_1(t) \sin x + a_3(t) \cos 3x + b_3(t) \sin 3x$. Assuming $\chi(x) = \cos 2x$, after the substituting to Eq. (1), we multiply the resulting expression by $\cos x$ and $\sin x$, and by $\cos 3x$ and $\sin 3x$, and for each case perform the integration over the spatial period 2π. The result is a set of equations for the amplitudes of the modes, which can be compactly expressed in the complex form as

$$\begin{aligned} \dot{c}_1 &= \mu_1 c_1 - \tfrac{1}{4}[3(|c_1|^2 + 2|c_3|^2)c_1 - 2Bc_3 + (3c_1^* c_3 - 2B)c_1^*], \\ \dot{c}_3 &= \mu_3 c_3 - \tfrac{1}{4}[3(|c_3|^2 + 2|c_1|^2)c_3 - 2Bc_1 + c_1^3], \end{aligned} \tag{3}$$

where the asterisk denotes complex conjugation, $c_1 = a_1 + ib_1$, $c_3 = a_3 + ib_3$, $\mu_1 = A - (1 - \kappa^2)^2$, $\mu_3 = A - (1 - 9\kappa^2)^2$, and $\kappa = \kappa(t)$, as before. Notice that the structure of the equations resembles that for the amplitude equations obtained for other models with hyperbolic attractors of Smale-Williams type [8,9,16].

Figure 4 illustrates the dynamics of the model (3). Observe the switchings after each next half-period $T/2$.

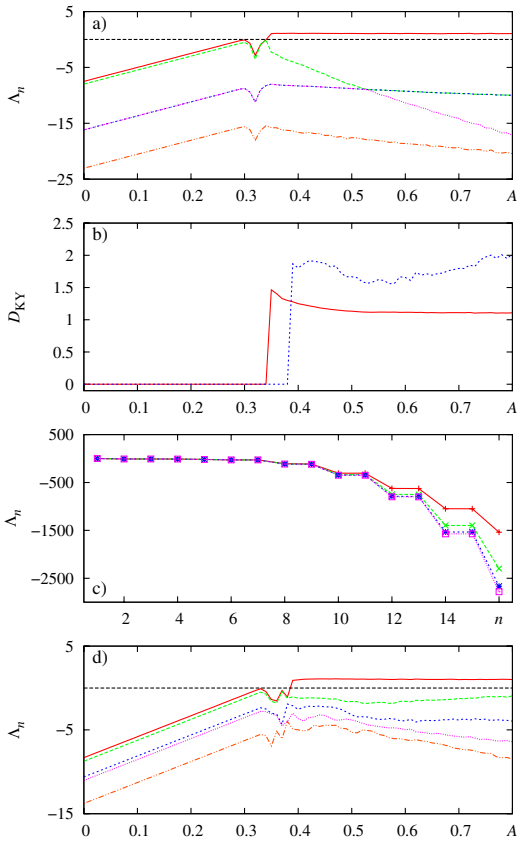

FIG. 3 (color online). (a) Five largest Lyapunov exponents vs A for the stroboscopic map of the system (1) at $t_n = (n + 1/4)T$, PBC. (b) Kaplan-Yorke dimension for PBC (solid line) and ZBC (dotted line). (c) PBC, first 16 exponents for different N: pluses, crosses, stars, and squares refer to $N = 64$, 128, 256, and 512, respectively. (d) ZBC, first five exponents. Other parameters are the same as in Fig. 1 for PBC and $B = 0.03$, $T = 25$, $L = 8\pi$, $N = 128$ for ZBC.

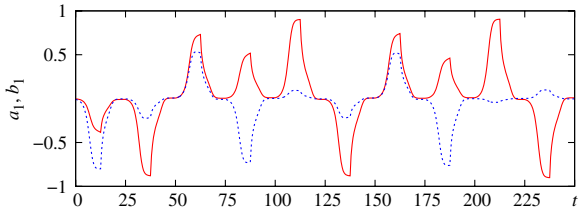

FIG. 4 (color online). Solution of Eq. (3) at $A = 0.6$, $B = 0.03$, $T = 25$. Solid (red) and dotted (blue) lines refer to $a_1 = \mathrm{Re}c_1$, and $b_1 = \mathrm{Im}c_1$, respectively.

Different heights of the humps of $\mathrm{Re}c_1$ and $\mathrm{Im}c_1$ arise due to the variations of the phases of c_1. The phases transform stroboscopically according to the triple expanding circle map; see Fig. 2(b) for the diagram for the phases computed as $\varphi_n = \arg[c_1(t_n)]$. The Lyapunov exponents evaluated for the stroboscopic map of the model (3) at $A = 0.6$, $B = 0.03$, $T = 25$ are $\Lambda = \{1.083, -12.5, -804.7, -806.5\}$, and the Kaplan-Yorke dimension is 1.09. Notice that the first exponent is close to ln3. The hyperbolicity test described above again shows that the expanding and contracting subspaces are almost perfectly orthogonal.

Now we intend to demonstrate that the hyperbolic chaos can be observed in geometries distinct from the ring one. In particular, let us examine simple zero boundary conditions (ZBC): $u(x, t) = 0$ for $x \leq 0$ and $x \geq L$, which could, in principle, block the mechanism of the chaotic transformation of the phases (because near the ends the spatial phase is dominated by the boundary conditions). However, computations show that such a blocking occurs only in short systems. If the length is large enough, patterns in the middle part of the system still interact in the same way as for PBC, while the parts close to the ends undergo deformations to fit ZBC; see Figs. 2(c) and 3(d) for $L = 8\pi$. The map for the spatial phases at the middle part of the system agrees well with the expected form. Moreover, there is a large parameter interval, where the system has a single positive Lyapunov exponent of value almost independent on A. At $A = 0.6$ the Lyapunov exponents are $\Lambda = \{1.047, -1.59, -3.92, -4.97, -6.16, \ldots\}$, and the Kaplan-Yorke dimension is 1.66. The hyperbolicity test shows pronounced separation of d_1 from the origin, although the distribution is wider ($0.93 < d_1 < 1$) than for PBC.

Summarizing, in this Letter we have shown how the hyperbolic chaotic dynamics can emerge in extended systems due to an interplay of spatial patterns with different wavelengths. In our model system the spatial phases of the patterns evolve in time according to the Bernoulli-type tripling map, and their dynamics is strongly and robustly chaotic, while the amplitudes behave in a rather regular manner. The mechanism of the hyperbolic chaos is similar to that in alternately excited oscillations, studied earlier [7]. In some respects, the chaotization of spatial phases appears to be easier for implementation (there is no necessity to have more than one involved subsystem). We have demonstrated the expected chaotic behavior in the partial differential equation of the Swift-Hohenberg type, and in the truncated model represented by a set of ordinary differential equations. It should be emphasized that the kind of dynamics we consider is not specific for the Swift-Hohenberg equation only. Ingredients needed for the phase multiplication mechanism, namely, the alternation of patterns due to parameter modulation, the nonlinearity, and the spatial inhomogeneity can be either found or created

in many spatially extended systems. As expected, these results open prospects for the search and constructing for hyperbolic chaos in pattern-formation for systems in fluid dynamics (Faraday ripples, convection rolls) and in reaction-diffusion systems (Turing structures, advection induced patterns) [12]. In the case of microfluidic systems [17,18], an interesting question for future studies is the effect of hyperbolic chaos on Lagrangian mixing properties.

The authors acknowledge support from the RFBR Grant No 11-02-91334 and DFG Grant No PI 220/14-1.

*p.kuptsov@rambler.ru

[1] A. A. Andronov, A. A. Vitt, and S. E. Khaikin, *Theory of Oscillators* (Dover Publications, New York, 2011), 2nd ed., p. 864.
[2] L. Shilnikov, Int. J. Bifurcation Chaos Appl. Sci. Eng. **7**, 1953 (1997).
[3] D. V. Anosov *et al.*, *Dynamical Systems IX: Dynamical Systems with Hyperbolic Behaviour*, Encyclopaedia of Mathematical Sciences Vol. 9 (Springer, New York, 1995), p. 242.
[4] S. Smale, Bull. Am. Math. Soc. **73**, 747 (1967).
[5] R. F. Williams, Publ. Math. Inst. Hautes Étud. Sci. **43**, 169 (1974).
[6] R. V. Plykin, Math. USSR Sb. **23**, 233 (1974).
[7] S. P. Kuznetsov, Phys. Rev. Lett. **95**, 144101 (2005).
[8] S. P. Kuznetsov and A. Pikovsky, Physica (Amsterdam) **232D**, 87 (2007).
[9] S. P. Kuznetsov, *Hyperbolic Chaos: A Physicist's View* (Higher Education Press, Bijing and Springer-Verlag, Berlin, Heidelberg, 2012), p. 336.
[10] S. P. Kuznetsov, Phys. Usp. **54**, 119 (2011).
[11] S. P. Kuznetsov and E. P. Seleznev, JETP **102**, 355 (2006).
[12] M. C. Cross and P. C. Hohenberg, Rev. Mod. Phys. **65**, 851 (1993).
[13] Also $\chi(x)$ can have the dominating fourth harmonic. In this case $\cos 4x \cos(3x + 3\varphi) = (1/2)\cos(x - 3\varphi) + \ldots$, so the map for the phase will be $\varphi_{n+1} = -3\varphi_n + \text{const}$. Under the variation of relative weights of the components $k = 2$ and $k = 4$ some transitions between the topologically distinct behaviors will occur.
[14] F. Ginelli, P. Poggi, A. Turchi, H. Chaté, R. Livi, and A. Politi, Phys. Rev. Lett. **99**, 130601 (2007).
[15] P. V. Kuptsov, Phys. Rev. E **85**, 015203 (2012).
[16] O. B. Isaeva, S. P. Kuznetsov, and E. Mosekilde, Phys. Rev. E **84**, 016228 (2011).
[17] N.-T. Nguyen and Z. Wu, J. Micromech. Microeng. **15**, R1 (2005).
[18] B. Stoeber, D. Liepmann, and S. J. Muller, Phys. Rev. E **75**, 066314 (2007).